

# Evaluation of the polarity of polyamide surfaces using the fluorescence emission of pyrene

Leonardo D.C. Baldi, Eduardo T. Iamazaki, Teresa D.Z. Atvars\*

*Departamento de Físico-Química, Instituto de Química, Universidade Estadual de Campinas, Caixa Postal 6154, 13084-971 Campinas, SP, Brazil*

Received 23 October 2006; received in revised form 16 January 2007; accepted 16 January 2007

Available online 2 February 2007

## Abstract

This paper reports the static and dynamic fluorescence emission of pyrene sorbed onto the surface of 6 different polyamides classified in two categories: AB (polyamide-6 and -11) or AAB (polyamide-6,6, -6,9, -6,10 and -6,12). Pyrene is a well known fluorescent probe for the polarity evaluation of different media for which the ratio of intensities of the vibronic bands ( $I_1/I_3$ ) decreases in less polar medium and the fluorescence decay from the singlet electronic excited state increases with decreasing polarity. The steady-state vibronic ratio  $I_1/I_3$  of the pyrene fluorescence emission decreases with decreasing polarity for polyamides AB but for polyamides AAB, this ratio undergoes a significant decrease for polyamides-6,9 compared with -6,6 but remains almost constant for polyamides-6,10 and -6,12. This shows that the steady-state fluorescence of pyrene is only sensitive to the polarity of sorption sites whose dimensions are similar to the van der Waals radius of the molecule. In contrast, fluorescence decays decrease with decreasing polarity of the polyamide from  $\tau_F = 250$  ns for polyamide-6,6 to  $\tau_F = 310$  ns for polyamide-6,12 and thus this parameter is always sensitive to the polarity of the medium. We also discuss the advantages of these spectroscopic methodologies that include their applicability to samples without any further sample manipulation and which is independent of their form, powder, pellet or film, and of their thicknesses and sizes.

© 2007 Elsevier Ltd. All rights reserved.

**Keywords:** Polyamides; Surface polarity; Pyrene; Fluorescence spectroscopy; Fluorescence decay

## 1. Introduction

The evaluation of surface properties is of fundamental interest for several different academic and technological aspects, such as phenomena related with adhesion [1,2], dyeing [3–5], painting, corrosion protection and several others [1,6]. Several techniques can be employed to determine surface properties, including spectroscopic methodologies using specular reflectance [7], measurements of interfacial tension and surface energy [1,6,8–10], atomic force microscopy [11,12], confocal laser scanning microscopy [13], near field microscopy [14], electron spin resonance [15] and measurements of zeta-potential [8–12]. The interaction strength between molecules and the surface is one of the properties that plays an important

role in these studies. The interaction strength is, in general, dependent on the nature of specific forces such as dipolar interactions, hydrophobic interactions, hydrogen bonding, electrostatic forces and in some other cases on the chemical bond generated between the surface and other chemical species [1,3,6,8–16].

For every goal, the development of methodologies able to determine the polarity of the surface is relevant. Although measurements of contact angle are well developed, this technique is complicated when the surface is not flat; one alternative methodology to measure surface polarity that overcomes this problem is fluorescence spectroscopy using fluorophores whose emission is sensitive to the polarity of the medium [17–21]. For this particular approach, samples can be utilised in the form of solutions or as powders, films, pellets, blocks of distinct sizes, etc. Nevertheless, the required condition is that the sample must be intrinsically luminescent or must contain an extrinsic fluorophore, which can be introduced by sorption

\* Corresponding author. Tel.: +55 19 3521 3078; fax: +55 19 3521 3023.

E-mail address: [tatvars@iqm.unicamp.br](mailto:tatvars@iqm.unicamp.br) (T.D.Z. Atvars).

or by chemical attachment [19,21–25]. For a non-intrinsically luminescent material the simplest way to extrinsically introduce the lumophore is through the sorption process, which can be done by techniques including: swelling by a non-solvent for the polymer [19,20,25], deposition by casting [19,20,25], spin-coating or dip-coating [26], self-assembly [27] or by vapor deposition when solvents should be avoided [19,28].

One interesting fluorophore is pyrene (Fig. 1), a strongly fluorescent molecule whose emission spectral profile and decay both depend on the polarity of the medium for solutions, microheterogeneous media or several types of surfaces [17–23,29,30]. For example, in a previous paper we showed that the ratio of vibronic fluorescence intensities and the emission decay of pyrene dissolved in several ethylene-*co*-vinyl acetate copolymers (EVA), either in the bulk or on the film surface, are linearly dependent on the vinyl acetate content in the copolymer [19]. EVA are copolymers whose ethylene and vinyl acetate segments are randomly distributed along the main chain and, consequently, the lengths of both segments have a broad size distribution. Thus, when sorbed onto the surface or dissolved in the bulk, pyrene is sensing an average polarity, without any correlation with the geometric distribution of the component blocks.

Different from EVA, polyamides are linear polymers or copolymers with a very well defined length of each block while the sequences of the blocks are also well defined (Scheme 1) [31,32]. They are produced by condensation reactions of diamines with dicarboxylic acids or by opening of ring lactams. Independent of the initial system, the sequence of the chain segments is very well defined in terms of their sequences and sizes. Depending on the processes, two types of polyamides can be produced: the polyamides AB, represented by number indices that describe the number of carbon atoms present in the aminocarboxylic acid (6 in the case of polyamide-6 and 11 in the case of polyamide-11); and polyamides AABB produced by polycondensation of diamines with dicarboxylic acids and described by number indices *x,y* (where *x* represents the number of carbon atoms present in the diamine and *y* the total number of carbon atoms present in the dicarboxylic block) [33]. For example, on going from polyamides-6,6 to -6,12 we increase the length of the dicarboxylic block from 6 to 12 carbons, maintaining 6 CH<sub>2</sub> units between the

diamine groups (Scheme 1). Because the size of the aliphatic chain between the polar groups increases with the increase of the index, we should expect that polymers with longer chains should be less polar.

The surface properties of polyamides have been studied by several techniques as an attempt to understand the dyeing process [3,8–10,13–16,32,34]. These studies have shown that not only dipolar and electrostatic forces play important role on the dye/sorption processes but that of dispersive forces are also important. Each one of these components must be determined in order to describe the total adhesion energy. Experiments of wettability using different liquids can be used to determine each of the interaction components [9]. Although this procedure allows a complete description of the interactions, it is time-consuming and, in several cases, the components are not completely independent.

This study is an attempt to describe the surface polarity of polyamide films with different structure using a simpler procedure that is based on measurements of both fluorescence spectra and fluorescence decay of electronically excited pyrene. Because the polyamide chains are linear we will correlate the measurements of the pyrene polarity parameters with the linear length of the polymer back-bone, which will be estimated by semi-empirical quantum mechanical calculations using the AM1 Hamiltonian method with molecular dynamics optimization using the software HyperChem™ 6.03 [35] (Scheme 1). This length was compared with the dimensions of the pyrene molecule, also estimated using the same methodology (Fig. 1).

## 2. Experimental

Pellets of polyamide-6, -11-, 6,6, -6,9, -6,10, -6,12 and polycaprolactone were purchased from Sigma–Aldrich and used as received. Formic acid (Merck, PA) was used. Pyrene (Sigma–Aldrich) was recrystallized twice from ethanol before use.

Polymer pellets were dissolved in formic acid and a powder was obtained by solvent evaporation. Then, samples were heated to near the melting point in an oven under a dynamic vacuum to erase the thermal history and to remove the residual solvent. After, they were pressed at room temperature using a load of 4 ton for 5 min at room temperature, forming a disc with about 1 cm of diameter, 1 mm thick. Onto the surface of every disc 10 drops of a pyrene in chloroform solution ( $10^{-4}$  mol L<sup>-1</sup>) were successively added. The pyrene was sorbed onto the sample surface after solvent evaporation. The amount of pyrene sorbed was followed by fluorescence spectroscopy and was considered adequate when the emission spectrum had sufficient intensity. The excitation spectrum was still sharp and a complete lack of excimer emission was observed [19,36]. The requirement of low concentration can be justified to avoid the inner-filter effect, self-absorption and re-emission, and several other possible types of intermolecular photophysical processes that may disturb the spectral profile as well as the fluorescence lifetimes. A very simple way to verify if this condition has been observed is by recording the

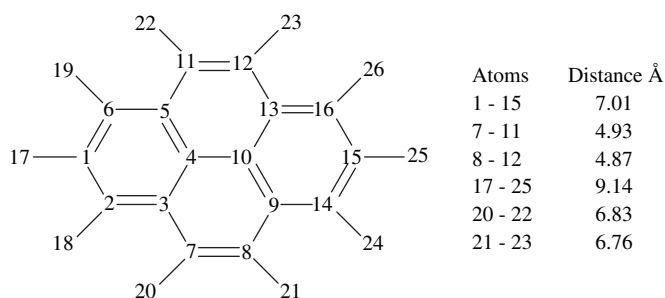


Fig. 1. Pyrene molecule. Linear length was estimated by semi-empirical quantum mechanical calculation with the AM1 Hamiltonian method with molecular dynamics optimization using the software HyperChem™ 6.03.

$\text{H}—[\text{—NH—(CH}_2\text{)}_5\text{—CO}]_n\text{—OH}$	polyamide -6
$\leftarrow 7.49 \text{ \AA} \rightarrow$	
$\text{H}—[\text{—NH—(CH}_2\text{)}_{10}\text{—CO}]_n\text{—OH}$	polyamide -11
$\leftarrow 12.24 \text{ \AA} \rightarrow$	
$\text{H}—[\text{—NH—(CH}_2\text{)}_x\text{—NH—CO—(CH}_2\text{)}_y\text{—CO—}]_n\text{—OH}$	polyamide -6,6
$\leftarrow 7.72 \text{ \AA} \rightarrow \leftarrow 6.10 \text{ \AA} \rightarrow$	
$\text{H}—[\text{—NH—(CH}_2\text{)}_x\text{—NH—CO—(CH}_2\text{)}_y\text{—CO—}]_n\text{—OH}$	polyamide -6,9
$\leftarrow 8.68 \text{ \AA} \rightarrow \leftarrow 10.12 \text{ \AA} \rightarrow$	
$\text{H}—[\text{—NH—(CH}_2\text{)}_x\text{—NH—CO—(CH}_2\text{)}_y\text{—CO—}]_n\text{—OH}$	polyamide -6,10
$\leftarrow 8.72 \text{ \AA} \rightarrow \leftarrow 11.31 \text{ \AA} \rightarrow$	
$\text{H}—[\text{—NH—(CH}_2\text{)}_x\text{—NH—CO—(CH}_2\text{)}_y\text{—CO—}]_n\text{—OH}$	polyamide -6,12
$\leftarrow 8.83 \text{ \AA} \rightarrow \leftarrow 13.31 \text{ \AA} \rightarrow$	
$\text{H}—[\text{—O—(CH}_2\text{)}_5\text{—CO—}]_n\text{—H}$	polycaprolactone
$\leftarrow 7.48 \text{ \AA} \rightarrow$	

Scheme 1. Molecular structures of some polyamides. Linear length was estimated by semi-empirical quantum mechanical calculation with the AM1 Hamiltonian method with molecular dynamics optimization using the software HyperChem™ 6.03.

excitation and emission spectra which must be composed of sharp bands [19].

Samples were characterized by dynamic scanning calorimetry (DSC) using a DSC 2910 TA Instruments calibrated with indium as standard. Samples initially at room temperature were cooled to 150 K using a rate of  $20 \text{ K min}^{-1}$  and then were heated at a rate of  $10 \text{ K min}^{-1}$  to above the melting point, cooled to 150 K and then a second heat cycle was run to above the melting point. The melting temperatures and enthalpies were determined using the data from the second heating cycle.

X-ray diffractograms were recorded on a Shimadzu-3A X-ray diffractometer, with a Cu K $\alpha$  source, current of 20 mA and voltage of 30 kV, in the range of  $2^\circ < 2\theta < 50^\circ$ . All the measurements were performed with part of the same sample used for the DSC measurements. Using the X-ray data we estimated the degree of crystallinity, which was determined by deconvolution of the diffraction peaks measured relative to the scattering band that defines the  $\chi_{\text{RX}}$  value. The area of the crystalline peaks was estimated by deconvolution with the software Origin 6.0. The crystallinity degrees from DSC and X-ray data were compared.

Steady-state fluorescence spectra were recorded using an ISS model PC1 spectrofluorimeter with a 300 W xenon

lamp. The excitation wavelength was  $\lambda_{\text{exc}} = 337 \text{ nm}$  and emission was recorded between 350 and 480 nm. Slits were selected for a spectral resolution of  $\pm 0.5 \text{ nm}$ . Spectra were recorded using front-face excitation and emission configurations with the sample held in a solid-state sample holder.

Fluorescence decays were recorded with the samples in a sealed quartz capillary under vacuum ( $10^{-4}$  torr) using the time-correlated single photon counting (TCSPC) technique in an Edinburgh Analytical Instruments nF900, operating with a pulsed H<sub>2</sub> lamp with a repetition frequency rate of 40 kHz,  $\lambda_{\text{exc}} = 337 \text{ nm}$  and  $\lambda_{\text{em}} = 393 \text{ nm}$ . Emission decay was recorded using front-face excitation and emission configurations with the sample held in a solid-state sample holder. The fluorescence decays  $F(t)$  were analyzed by deconvolution of the lamp pulse recorded using a solution of LUDOX™ (DuPont) with the impulse response of the sample. The fluorescence decays,  $F(t)$ , were analyzed by the exponential series method (ESM) fitting the experimental curves with two-exponential functions. Freely adjustable positive  $B_i$  values represent the weight fraction for each exponential decay. The search for the best fit uses the Marquardt algorithm to minimize the reduced  $\chi^2$  (goodness of fit). Fits are considered acceptable

when  $\chi^2 < 1.2$  and the distributions in the residual plots were randomly distributed.

Sorption of pyrene on the sample surface is demonstrated by epifluorescence microscopy (EFM) performed using an inverted Leica DM IRB microscope employing a mercury arc lamp (HBO-100 W) for UV–vis excitation in the wavelength range of 330–380 nm selected by optical filters [23,37]. The emission image was selected from the excitation beam by a dichroic mirror ( $\lambda_{\text{exc}} > 410$  nm). Objective magnifications of 50 $\times$  were used and the images were taken with a Samsung SDC-311 digital camera and processed by Linksys v. 2.38 software.

To provide a sorption model for the experimental results a theoretical study was undertaken using quantum mechanical calculations with AM1 Hamiltonian for the optimization of the geometry of one monomer unit of every polyamide structure. We also simulated the geometry of two linear monomer units and thus we searched for bimolecular aggregates with the framework of classical molecular mechanics (MM). This was carried out with the molecular dynamics optimization of the software HyperChem™ 6.03.

### 3. Results and discussion

#### 3.1. Polymer characterization

Polymer samples were physically characterized by both DSC and X-ray diffraction [38,39]. From the DSC data we determined the melting temperature using the value of the endothermic peak and these were similar to those reported in the literature [31,32]. Measurements with and without pyrene sorbed onto the surface did not modify the melting temperature.

Diffraction patterns also showed that the samples are crystallized in the most thermally stable unit cell and they were not deformed or modified by pyrene deposition on the sample surface. The degree of crystallinity of every polyamide sample was determined by X-ray diffraction patterns using the ratio between the areas of the crystalline peaks divided by the total area. Our values are also very similar to those reported in the literature [31] and are in the range from 59 to 61%.

Sorption of pyrene on the polymer samples was demonstrated by epifluorescence optical microscopy. For example, a sample of pyrene sorbed onto the polyamide-6,10 surface shows an image colored by blue when ultraviolet is used for excitation due to the fluorescence of pyrene (Fig. 2). Similar behavior was observed for other the samples and figures have been omitted. Samples without pyrene are non-fluorescent when employing UV excitation irradiation.

We noted that the residual emission of the polyamides under our experimental conditions ( $\lambda_{\text{exc}} = 350$  nm emitted by a conventional lamp and spectra recorded using front-face excitation) is very weak for samples without pyrene. Therefore, our data can be considered as being originated only from the pyrene molecules.

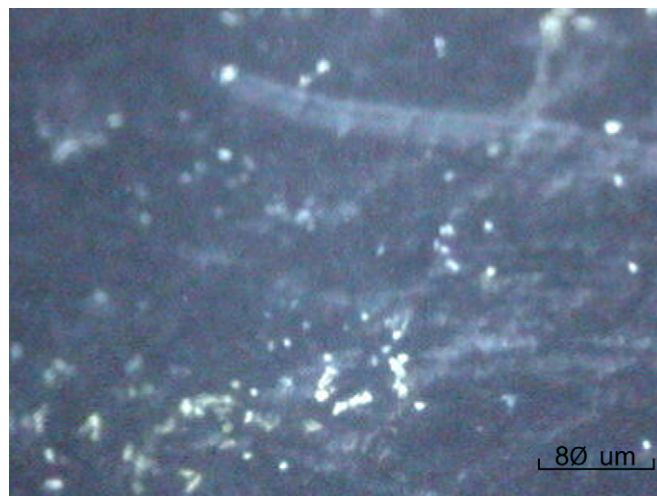


Fig. 2. Epifluorescence optical microscopy of a polyamide-6,10 sample with pyrene on its surface.  $\lambda_{\text{exc}} > 350$  nm.

#### 3.2. Steady-state fluorescence emission

Steady-state fluorescence spectra of pyrene sorbed onto the surface of polyamides using an excitation wavelength of  $\lambda_{\text{exc}} = 337$  nm are in Fig. 3. In general, these spectra are composed of a vibronically structured band characteristic of the isolated pyrene molecules [17–22,29]. No excimer emission was detected.

The  $I_1/I_3$  vibronic intensity ratios were determined from the fluorescence spectra where the intensities  $I_1$  and  $I_3$  correspond to the vibronic bands at  $\lambda_{\text{em}} = 370$ – $374$  nm and  $\lambda_{\text{em}} = 380$ – $384$  nm, respectively. The values given in Table 1 were determined as an average of two sets of emission spectra, each set was recorded using two different parts of two samples. The average ratio of one sample was averaged with the average ratio of the second sample. According to the pyrene polarity scale (py-scale), a greater  $I_1/I_3$  intensity ratio can be attributed to a more polar medium and vice-versa [17,18,21]. Therefore, as we can see from Table 1, for AB-type polyamides such as polyamide-6 and polyamide-11, this ratio changes from 1.41 to 1.27, demonstrating that, for the shorter aliphatic chain, pyrene senses a more polar medium, as expected. Comparing this with solvents, the value of the vibronic ratio for polyamide-6 is similar to that of solvents such as 2-methylcyclohexanone, 2-heptanone, *n*-heptanone and 1,2-butanediol, whose values are in the range 1.41–1.45, while the polarity of polyamide-11 is similar to 3-octanone and 2-methyl-1,4-pentanediol, whose ratio is in the range 1.26–1.31 [17,18].

In the same way, for the polyamides of the AABB type (polyamide-6,6, -6,9, -6,10 and -6,12), the greatest polarity was observed for the polyamide containing the smaller aliphatic segment from the carboxylic acid block (polyamide-6,6) (Table 1). For the aliphatic segments from polyamide-6,6 to polyamide-6,12, we observe that the  $I_1/I_3$  ratio decreases from polyamide-6,6 (1.44) to polyamide-6,9 (1.31) but then remains constant for the other polyamides (1.29–1.31). This result suggests that there is a critical relative distance between

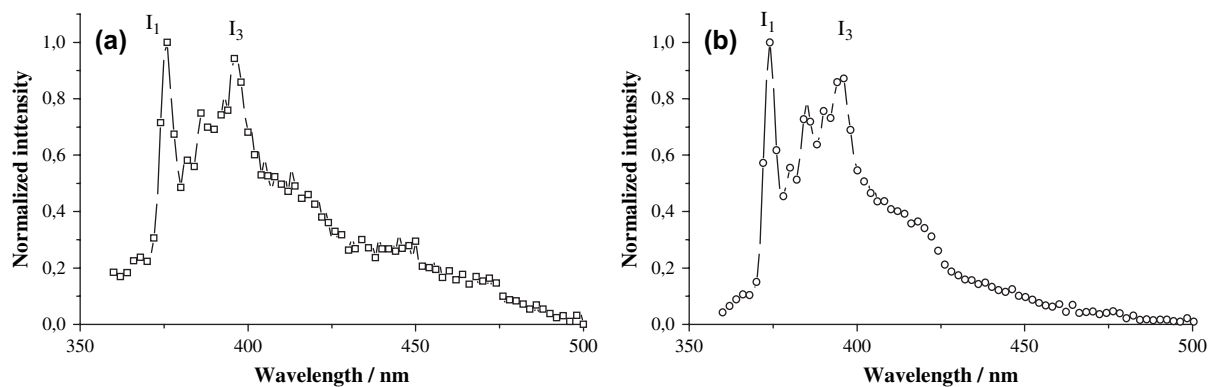


Fig. 3. Normalized steady-state fluorescence spectra of pyrene sorbed onto the surface of: (a) polyamide-6,6 and (b) polyamide-6,12. Intensity has been normalized for the band at 371–374 nm.  $\lambda_{\text{exc}} = 337$  nm.

the polar groups and the position of the pyrene molecules, above which the vibronic ratio is not an adequate parameter for the py-scale. Comparing with solvents, these values of vibronic ratio indicates that polyamide-6,6 has a polarity similar to 2-methylcyclohexanone, 2-heptanone and 1,4-butanediol while polyamide-6,9, and polyamide-6,10 are similar to 3-octanone and 2-methyl-1,4-pentanediol [17,18]. It is worth noting that above a certain length of the aliphatic chain, somewhere between 6 and 9  $\text{CH}_2$  groups, the vibronic ratio becomes almost constant and independent of the number of  $\text{CH}_2$  of the aliphatic group. In other words, the vibronic ratio of the pyrene fluorescence is unable to distinguish differences of polarity for polyamide-6,9, -6,10 and -6,12. This behavior is different from that observed for EVA and copolymers with small amounts of ethyl acetate show differences in the vibronic ratio [19].

The fluorescence lifetimes of pyrene sorbed onto the polyamide samples were determined by deconvolution of the lamp pulse signal (fast pulse). A typical example of these signals is shown in Fig. 4 for pyrene sorbed onto polyamide-6 (others' spectra have been omitted). The lifetime of the pyrene fluorescence was determined by deconvolution of the pulse of the lamp (fast pulse) and curve of the sample (slower decay). After deconvolution the decay was fitted using exponential functions. In general, good fits can be obtained for pyrene sorbed onto the polyamide surfaces using a monoexponential function and the lifetimes are shown in Table 1.

The decay of pyrene fluorescence is always faster for the more polar medium as expected [17–20,21,23]. What we

observe here is that for each specific set of polyamide (AB or AABB), the lifetime decreases for polymers with shorter aliphatic chains, as expected for more polar media. It is noteworthy that, while the vibronic ratio cannot make a distinction for the polarity of polyamides-6,9, -6,10 and -6,12, the decays are different and follow the expected decrease as the length of the aliphatic chain decreases.

In an attempt to explain the sensitivity of pyrene to the polarity of the polyamide samples, we are using a very simple approach assuming two neighborhood chains are maintained together by hydrogen bonding. Once together, they form a cavity which may be occupied by pyrene molecules (Fig. 5). It is well known that pyrene has a hydrophobic character and shows a tendency to occupy more apolar cavities [17–21]. Consequently, the preferential sorption sites should be those near the aliphatic chains and this is the reason for the similarity among the values for the py-polarity observed and the values for molecules with relatively lower polarity observed with our data.

If our model can represent the sites of the sorption for pyrene on polyamide sample surfaces, we should expect that the

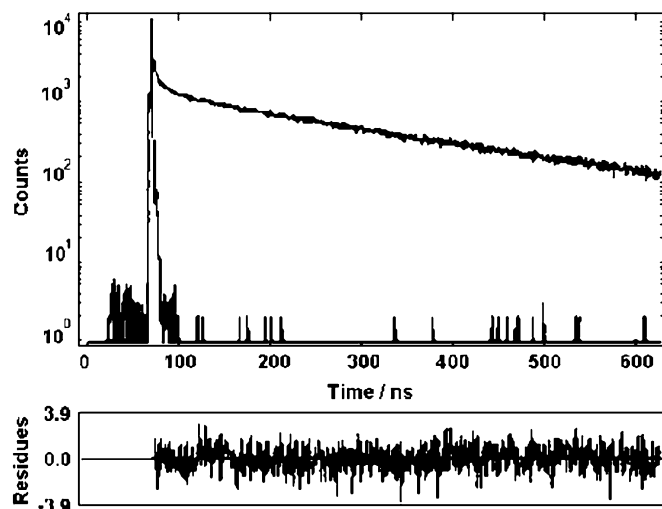


Fig. 4. Fluorescence lifetime spectrum of pyrene sorbed onto the surface of polyamide-6.

Table 1  
Vibronic ratio  $I_1/I_3$  and lifetime  $\tau_F$  (ns) of the fluorescence emission of pyrene sorbed onto the surface of several polyamides

Polyamide	Vibronic ratio $I_1/I_3$	$\tau_F$ (ns)
-6	$1.41 \pm 0.04$	$260 \pm 1$
-11	$1.27 \pm 0.03$	$276 \pm 3$
-6,6	$1.44 \pm 0.02$	$250 \pm 3$
-6,9	$1.31 \pm 0.03$	$276 \pm 2$
-6,10	$1.30 \pm 0.04$	$296 \pm 3$
-6,12	$1.29 \pm 0.03$	$310 \pm 3$
Polycaprolactone	$1.15 \pm 0.02$	$265 \pm 5$

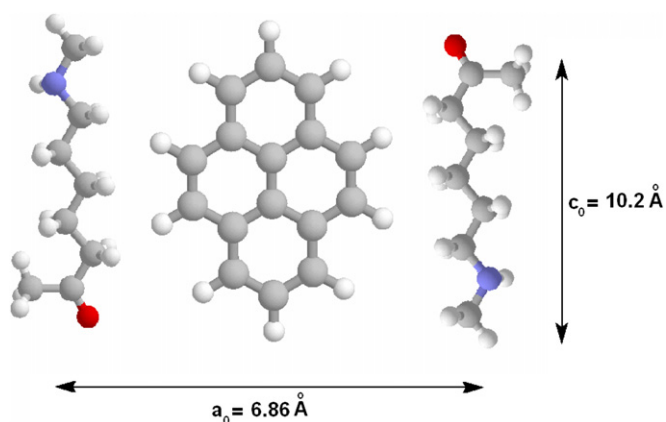


Fig. 5. Schematic dimensions of the box formed by chains of polyamide-6, whose cavity could contain a pyrene molecule.

dimensions of the cavities would be similar or larger than the pyrene dimensions (Fig. 1). Therefore, we estimated the linear lengths of the polyamide chains using a semi-empirical methodology of molecular orbital calculations with the Hamiltonian AM1 to optimize the special geometry [35] (Scheme 1). In addition, we estimated using molecular mechanics that the interchain distance is around 6.86 Å between dicarboxylic groups and 6.90 Å between diamine groups, which are approximately the same as the shorter axis distance of the pyrene molecule (Fig. 1).

For pyrene, we determined that the dimension of its longer molecular axis (distance between the atoms 17 and 25) is 9.14 Å, which is longer than the longer linear axis of polyamide-6 (7.49 Å) and shorter than that of polyamide-11 (12.24 Å) (Scheme 1). Therefore, we should expect that pyrene will sense a less polar environment when sorbed onto the polyamide-11 surface than onto polyamide-6. When comparing polyamide-6 with polycaprolactone, which has almost the same linear dimensions, our photophysical data suggest that photoluminescence is less polar since the vibronic  $I_1/I_3$  is lower and the lifetime is longer (Table 1).

From the spectroscopic point of view, polyamide-6 and polycaprolactone can be considered Shpol'skii matrices for pyrene, that is, matrices presenting cavities with similar dimensions to the molecular luminescent probes resulting in a fluorescence spectrum with maximum vibronic resolution [28,36]. In other words, there is good correspondence between the size and the form of the "solvent cage" and the molecular dimensions of the molecule-guest. The polar groups of the matrix are the nearest possible to the pyrene molecules. In the case of polyamide, whose monomer has a larger linear length than that of the molecule-guest (pyrene), the polar groups are more distant and the medium in which molecule-guest situated is less polar. These phenomena reflect on the values of the relationship of vibronic intensities and on the fluorescence lifetime of pyrene.

In the case of polyamides AABB, the analysis is similar. For example, the carboxylic chains of polyamide-6,6 form cages with dimensions of 7.72 Å for the diamine segments and 6.10 Å for the carboxylic acid segments with an interchain

distance of 6.86 Å. In both cavities pyrene molecules can be accommodated. Because these cavities have dimensions similar to those for polyamide-6, the polarity measured by the py-scale was almost the same.

When we move from polyamide-6,6 to polyamide-6,9, there is a larger increase of the length of the dicarboxylic segments, whose linear length changes from 6.10 Å for polyamide-6,6 to 10.12 Å for polyamide-6,9. The increase is due to the increase of the length of the apolar aliphatic chain and the consequence is that pyrene is located in a less polar environment that then explains the observed photophysical changes. Compared with the dimensions of the pyrene molecule, the cavity of the polyamide-6,9 is larger than that required for a quasi-linear emission spectrum. The increase of the aliphatic chain for polyamide-6,10 and for polyamide-6,12 occurs only for the dicarboxylic chain, since the amide component is the same (Scheme 1). Although the size increases, the vibronic ratio for the pyrene emission in these polyamides is almost constant.

From the analysis of the dimensions of the cavities there are two possible explanations for the photophysical behavior of pyrene sorbed onto the polyamide surfaces. One is that the cavity where these molecules are located is the amide domain that has almost the same dimensions for polyamide-6,9, -6,10 and -6,12. Considering that pyrene is sensing domains of the same polarity, both vibronic ratios and fluorescence lifetimes must be the same, for all polymers which has not been observed. Actually, we observed that the vibronic ratio is almost constant but the lifetimes increase with the decrease of the polarity. Therefore, we must consider an additional hypothesis, which is that the pyrene molecules, in addition to sensing the polarity of the amide domains, is also sensing the dicarboxylic regions which are changing along the polyamide series. We suspect that the reason for the constant value of the vibronic ratio that parameter has a shorter-distance dependence because it results from electron–phonon coupling [40–43] with the matrix while the lifetime is a dynamic parameter dependent on the coupling between the simultaneous dipolar relaxation of the matrix and of the probe. Therefore, because the static photophysical parameter depends on the relative dimension of the cavity and the probe, the fluorescent molecule can only sense cavities whose dimensions are similar to its van der Waals radius. As a consequence, the lifetime is a more useful tool for sensing polarity in the case of pyrene molecules.

#### 4. Conclusion

We showed here that pyrene is a sensor for polarity of polyamides belonging to either the AB or the AABB types. This molecular sensor in the excited singlet state undergoes photophysical processes whose steady state and dynamic properties respond to the environmental characteristics both in solution and in the solid state. However, we observed that the ratio of the vibronic intensities  $I_1/I_3$  of the fluorescence band is a good parameter for sorption cages of similar dimensions as the molecular van der Waals radius while the lifetime has

more universal polarity dependence. Smaller lifetimes were obtained for the most polar polyamides of the two families. Because of the relationship between the size of the pyrene molecule and the size of the polyamide cavity we could conclude that the steady-state emission vibronic ratio of pyrene is a short-range parameter, in other words, above a certain distance it does not respond to its environment. Nevertheless, the fluorescence lifetimes still respond to the distinct polarity of the polyamides.

An additional advantage of the fluorescence decay compared with steady-state emission is related to the presence of some residual emission of the polymer. In particular, for polyamide-6 an emission centered at 415 nm was reported for  $\lambda_{\text{exc}} = 345$  nm. If some residual emission (not observed under our experimental conditions) is present, it might disturb the band at  $\sim 390$  nm, increasing its relative intensity. Therefore, the observed vibronic ratio should be smaller than that effectively expected. On the other hand, because the pyrene lifetime is much longer than that for other aromatic compounds, its decay should not be disturbed by other eventual faster emission signals [18–20,36].

In a previous work we showed that fluorescence spectroscopy may be used to determine polarity using the concept of the py-scale for polymer films of distinct copolymers [19]. Here we showed that this methodology can also be employed for polymers in powder form, indicating that the methodology has no apparent geometric restrictions, being applied for materials with higher light scattering properties, such as powders.

## Acknowledgments

The authors thank FAPESP, FAEPEX-Unicamp, CNPq, CAPES and MCT/CNPq/IMMP for financial support and fellowships. We also acknowledge Prof. Carol Collins for useful discussions.

## References

- [1] Adamson AW, Gast AP. *Physical chemistry of surfaces*. 6th ed. New York: Wiley; 1997.
- [2] Crippa PR, Fornes JA, Ito AS. Photophysical properties of pyrene in interaction with the surface of melanin particles. *Colloids and Surfaces B: Biointerfaces* 2004;35(2):137–41.
- [3] Jesionowski T, Binkowski S, Krysztafkiewicz A. Adsorption of the selected organic dyes on the functionalized 14 surface of precipitated silica via emulsion route. *Dyes and Pigments* 2005;65(3):267–79.
- [4] Venkataraman K. *The chemistry of synthetic dyes*, vol. 1. New York: Academic Press; 1952.
- [5] Rys P, Zollinger H. *Fundamentals of the chemistry and application of dyes*. London: Wiley-Interscience; 1972.
- [6] Good RJ, van Oss CJ. In: Schrader ME, Loeb GI, editors. *Modern approaches to wettability: theory and applications*. New York: Plenum Press; 1992.
- [7] Koenig JL. *Spectroscopy of polymers*. 2nd ed. Amsterdam, New York: Elsevier; 1999.
- [8] Espinosa-Jimenez M, Padilla-Weigand R, Ontiveros-Ortega A, Perea-Carpio R, Ramos-Tejada MM, Chibowski E. Investigation of the polyamide 6,6 dyeing process with Acid Blue 45 dye. Part I. Thermodynamics of Acid Blue 45 adsorption. *Journal of Adhesion Science and Technology* 2002;16(3):285–301.
- [9] Espinosa-Jimenez M, Padilla-Weigand R, Ontiveros-Ortega A, Perea-Carpio R, Ramos-Tejada MM, Chibowski E. Investigation of the polyamide 6,6 dyeing process with Acid Blue 45 dye. Part II. Surface free energy, zeta potential and dye/polyamide interactions. *Journal of Adhesion Science and Technology* 2002;16(3):303–16.
- [9] Tate ML, Kamath YK, Wesson SP, Ruetsch SB. Surface energetics of nylon 66 fibers. *Journal of Colloid and Interface Science* 1996;177(2):579–88.
- [10] Espinosa-Jimenez M, Padilla-Weigand R, Ontiveros-Ortega A, Ramos-Tejada MM, Perea-Carpio R. Interpretation of colloidal dyeing of polyester fabrics pretreated with ethyl xanthogenate in terms of zeta potential and surface free energy balance. *Journal of Colloid and Interface Science* 2003;265(2):227–33.
- [11] Patrick HN, Warr GG, Manne S, Aksay IA. Surface micellization patterns of quaternary ammonium surfactants on mica. *Langmuir* 1999;15(5):1685–92.
- [12] Kovacs L, Warr GG. Changes in the adsorbed layer structure of cationic surfactants on mica induced by adsolubilized aromatic molecules. *Langmuir* 2002;18(12):4790–4.
- [13] De Clerck K, Van Oostveldt P, Rahier H, Van Mele B, Westbroek P, Kiekens P. Variations in diffusion coefficient of disperse dyes in single PET fibres: monitored and interpreted by confocal laser scanning microscopy. *Polymer* 2005;46(1):101–8.
- [14] Schaller RD, Lee LF, Johnson JC, Haber LH, Saykally RJ, Viece J, et al. The nature of interchain excitations in conjugated polymers: spatially-varying interfacial solvatochromism of annealed MEH-PPV films studied by near-field scanning optical microscopy (NSOM). *Journal of Physical Chemistry B* 2002;106(37):9496–506.
- [15] Esumi K, Otsuka H, Meguro K. Study of surfactant layer on alumina by ESR spin probe technique. *Journal of Colloid and Interface Science* 1990;136(1):224–30.
- [16] Aloulou F, Boufi S, Belgacem N, Gandini A. Adsorption of cationic surfactants and subsequent adsolubilization of organic compounds onto cellulose fibers. *Colloid and Polymer Science* 2004;283(3):344–50.
- [17] Kalyanasundaram K, Thomas JK. Environmental effects on vibronic band intensities in pyrene monomer fluorescence and their application in studies of micellar systems. *Journal of the American Chemical Society* 1977;99(7):2039–44.
- [18] Dong DC, Winnik MA. The py-scale of solvent polarities. *Canadian Journal of Chemistry/Revue Canadienne de Chimie* 1984;62(11):2560–5.
- [19] Prado EA, Yamaki SB, Atvars TDZ, Zimerman OE, Weiss RG. Static and dynamic fluorescence of pyrene as probes of site polarity and morphology in ethylene-co-(vinyl acetate) (EVA) films. *Journal of Physical Chemistry B* 2000;104(25):5905–14.
- [20] Neumann MG, Schmitt CC, Iamazaki ET. A fluorescence emission study of the formation of induced premicelles in solutions of polyelectrolytes and ionic surfactants. *Journal of Colloid and Interface Science* 2003;264(2):490–5.
- [21] Thomas JK. Characterization of surfaces by excited-states. *Journal of Physical Chemistry* 1987;91(2):267–76.
- [22] Zimerman OE, Weiss RG. Static and dynamic fluorescence from alpha, omega-di(1-pyrenyl)alkanes in polyethylene films. Control of probe conformations and information about microstructure of the media. *Journal of Physical Chemistry A* 1998;102(28):5364–74.
- [23] de Andrade ML, Atvars TDZ. Dynamic and static fluorescence spectroscopy applied to miscibility of poly(*n*-butyl methacrylate-co-styrene) with polystyrene and morphological analysis by epifluorescence microscopy. *Journal of Physical Chemistry B* 2004;108(13):3975–84.
- [24] de Deus JF, Andrade ML, Atvars TDZ, Akcelrud L. Photo and electroluminescence studies of poly(methyl methacrylate-co-9-anthryl methyl methacrylate). *Chemical Physics* 2004;297(1–3):177–86.
- [25] Talhavini M, Atvars TDZ, Schurr O, Weiss RG. Translocation of fluorescent probes upon stretching low-density polyethylene films. Comparison between “free” and covalently-attached anthryl groups. *Polymer* 1998;39(14):3221–32.
- [26] Notley SM, Eriksson M, Wagberg L, Beck S, Gray DG. Surface forces measurements of spin-coated cellulose thin films with different crystallinity. *Langmuir* 2006;22(7):3154–60.

- [27] dos Santos DS, Mendonça CR, Balogh DT, Dhanabalan A, Giacometti JA, Zilio SC, et al. Optical storage in mixed Langmuir–Blodgett (LB) films of Disperse Red 19. *Synthetic Metals* 2001;121(1–3):1479–80.
- [28] Coltro L, Dibbern-Brunelli D, Elias CAB, Talhavini M, de Oliveira MG, Atvars TDZ. Fluorescence-spectra of anthracene dissolved in vinylic and olefinic polymers. *Journal of the Brazilian Chemical Society* 1995;6(2):127–33.
- [29] Jay J, Johnston LJ, Scaiano JC. Quenching of pyrene fluorescence by cupric ions in micellar solution — effect of quenching on the polarity reported by the probe. *Chemical Physics Letters* 1988;148(6):517–22.
- [30] Kaufman VR, Avnir D. Structural-changes along the sol–gel–xerogel transition in silica as probed by pyrene excited-state emission. *Langmuir* 1986;2(6):717–22.
- [31] Kohan I. *Nylon plastics handbook*. Cincinnati: Hanser/Gorden Publ., Inc.; 1995.
- [32] Reimschuessel H. *Handbook of fiber science and technology*. In: Lewin M, Pearce EM, editors. *Fiber chemistry*, vol. IV. New York: Marcel Dekker; 1985.
- [33] Fox RB. Naming organic polymers. II. Structure-based polymer nomenclature. *Journal of Chemical Education* 1974;51(2):113–5.
- [34] Savarino P, Parlati S, Buscaino R, Piccinini P, Barolo C, Montoneri E. Effects of additives on the dyeing of polyamide fibers. Part II. Methyl- $\beta$ -cyclodextrin. *Dyes and Pigments* 2006;69(1–2):7–12.
- [35] Schleyer PVR, editor. *Encyclopedia of computational chemistry*. Chester: John Wiley; 1998.
- [36] Lakowicz JR. *Principles of fluorescence spectroscopy*. 2nd ed. New York: Kluwer Academic & Plenum Publications; 1999.
- [37] De Andrade ML, Atvars TDZ. Photophysical study in blends of poly(alkyl methacrylate-*co*-styrene)/polystyrene. *Macromolecules* 2004;37(24):9096–108.
- [38] Rabek F. *Experimental methods in polymer chemistry: physical principles and applications*. New York: Wiley-Interscience; 1987.
- [39] Alexander LE. *X-ray diffraction methods in polymer science*. New York: Wiley-Interscience; 1969.
- [40] Thijssen HPH, Völker S. Spectral hole burning in semicrystalline polymers between 0.3-K and 4.2-K. *Journal of Chemical Physics* 1986;85(2):785–93.
- [41] Geldof PA, Rettschn RP, Hoytink GJ. Vibronic coupling and radiative transitions. *Chemical Physics Letters* 1971;10(5):549–53.
- [42] Vigil MR, Bravo J, Atvars TDZ, Baselga J. Photochemical sensing of semicrystalline morphology in polymers: pyrene in polyethylene. *Macromolecules* 1997;30(17):4871–6.
- [43] Vigil MR, Bravo J, Baselga J, Yamaki SB, Atvars TDZ. Micromorphology and relaxation processes of low density polyethylene probed by fluorescence spectroscopies. *Current Organic Chemistry* 2003;7(3):197–211.